Supramolecular Synthesis through Dihydrogen Bonds: Self-Assembly of Controlled Architectures from $NaBH_4$ · Poly(2-hydroxyethyl)cyclen Building Blocks

Radu Custelcean,*[a] Mircea Vlassa,[b] and James E. Jackson*[a]

Abstract: A systematic investigation of molecular structures/supramolecular organization relationships in dihydrogen-bonded complexes comprising $NaBH_4$ and poly-2-hydroxyethyl-cyclen (poly-HEC) building blocks is reported. Like in the prototype compound **1**, a $(NaBH_4$-poly-HEC$)_2$ dimeric arrangement has been found in the analogous structures **3** and **5**, but not in compound **2**, which lacks dihydrogen bonds. The exact connectivity of the dimers is determined by a complex interplay of noncovalent interactions such as OH···HB dihydrogen bonds, OH···O conventional hydrogen bonds, Na–O and Na–N coordinative bonds, and dispersion interactions. The persistent recurrence of this general supramolecular motif permits controlled assembly of extended networks with desired architectures, by the use of appropriate spacers for linking the dimers, as demonstrated by the solid-state structure of **7**. Additionally, the intrinsic solid-state reactivity of these dihydrogen-bonded networks makes this approach a promising strategy for the rational construction of functional extended covalent solids.

Keywords: crystal engineering · hydrogen bonds · noncovalent interactions · self-assembly · supramolecular chemistry

Introduction

There is increasing interest in the employment of hydrogen bonds in the supramolecular synthesis of new materials with desired structures and properties.[1] The advantage of using these weak but directional interactions is that they allow rapid self-organization of molecular building blocks into extended regular structures, which represents a very efficient process compared with conventional synthesis using covalent bonds. Recently, a special type of hydrogen bonding (dihydrogen bonding), in which a σ M–H bond (M = Al, B, Ga, Ir, Mo, Mn, Os, Re, Ru, W) acts as the proton acceptor, has been the subject of numerous investigations.[2] Geometrically, dihydrogen bonding is generally characterized by short H···H contact distances (typically 1.7–2.2 Å) and strongly bent AH···H–M angles (typically 90–135°). Its nature is mostly electrostatic, although a weak covalent contribution can sometimes be found.[2a] With strength and directionality comparable with those found in conventional hydrogen bonding, this hydridic-to-protonic interaction can also direct crystal packing, offering potential utilities in crystal engineering.[3] The additional feature that makes these unconventional hydrogen bonds particularly interesting is their ability to react in the solid state by H_2 loss, trading the weak H···H interactions for strong covalent bonds (Scheme 1). This opens new avenues to the rational assembly of extended covalent materials with controlled architectures.[4] We have employed A–H···H–B (A = O, N) dihydrogen bonds in the construction of zero-, one-, two-, and three-dimensional networks with various motifs, and have shown that some of these systems can react topochemically to form novel covalent materials that were otherwise not accessible from solution.[4a–d] While the resulting products of these topochemical transformations were generally amorphous, very recently we demonstrated that judicious engineering of the starting dihydrogen-bonded

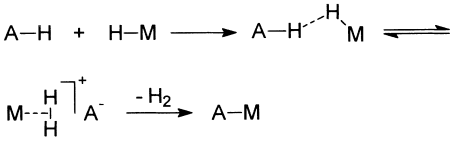

Scheme 1.

[a] Dr. R. Custelcean,[+] Prof. J. E. Jackson
Department of Chemistry, Michigan State University
East Lansing, MI 48824 (USA)
E-mail: custelce@cems.umn.edu, jackson@cem.msu.edu

[+] Present Address:
Department of Chemical Engineering and Materials Science
University of Minnesota, 421 Washington Ave. SE
Minneapolis, MN 55455 (USA)

[b] Prof. M. Vlassa
Department of Chemistry, Babes-Bolyai University
11 Arany Janos Street, Cluj-Napoca, 3400 (Romania)

0947-6539/02/0801-0302 $ 17.50+.50/0 *Chem. Eur. J.* **2002**, *8*, No. 1

crystals may allow preservation of crystallinity during the O–H···H–B to O–B conversion.[4a] Thus, solid-state decomposition of the $NaBH_4 \cdot THEC$ (THEC = *N*,*N*′,*N*″,*N*‴-tetrakis-(2-hydroxyethyl)cyclen) (**1**) dihydrogen-bonded complex led to a crystalline covalent product by a crystal-to-crystal process. It appears that this outcome is the result of self-assembly into large globular hydrogen-bonded $(NaBH_4 \cdot THEC)_2$ dimers (Figure 1), whose close packing in the initial crystal minimizes the shrinkage of the unit cell during decomposition.

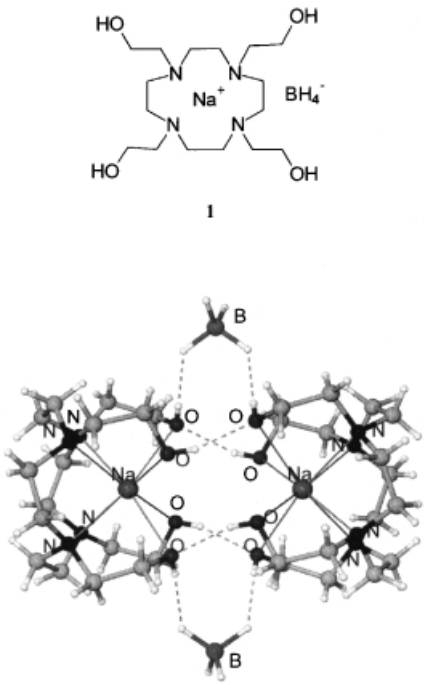

Figure 1. Structure of $NaBH_4 \cdot THEC$ (**1**) and its self-assembly into dihydrogen-bonded dimers.

We seek a generalization of this strategy that will eventually lead to the controlled assembly of extended crystalline covalent networks. Further elaboration of the dihydrogen-bonded building blocks present in **1**, which proved to possess the required geometrical and solid-state reactivity prerequisites, appears to be the most potentially successful approach toward this objective. However, an important and necessary condition is that the dihydrogen-bonded dimeric motif observed in **1** be robust enough to survive substantial modifications in molecular structure. For a truly rational approach toward covalent solids, adequate control over the supramolecular arrangement of the initial dihydrogen-bonded structures is first required. While crystal engineering with conventional hydrogen bonds is now a well-explored field,[1] no systematic study employing the less common dihydrogen bonds has been reported to date. This report presents our efforts directed toward the understanding of the relationships between molecular structures and supramolecular organizations in sodium borohydride complexes with poly-HEC (HEC = 2-hydroxyethylcyclen) ligands. We show that despite the high flexibility of these ligands, the H···H interactions to the BH_4^-, assisted by preorganization of the OH proton donor groups by complexation to Na^+, induce persistent recurrence of a $(NaBH_4 \cdot poly\text{-}HEC)_2$ general dimeric motif, which may ultimately be exploited for the assembly of extended dihydrogen-bonded systems with controlled architectures.

Results and Discussion

The high flexibility of THEC does not recommend it as a reliable building block for the construction of supramolecular networks with predictable architectures. However, the coordination of alkali metal cations locks the ligand into a conformation with all four hydroxyethyl arms projecting to the same side of the azacrown ring, leading to an almost cubic disposition of the nitrogen and oxygen atoms.[4a,5] This geometry favors the self-assembly of **1** into dihydrogen-bonded closed loop dimers, which to date appears to be the most promising arrangement for the preservation of crystallinity through solid-state dihydrogen-to-covalent bonding conversions.

The dimers in **1** are held together by four conventional OH···O hydrogen bonds, complemented by four orthogonal OH···HB dihydrogen bonds (Figure 1). To explore the role of the latter interactions in the dimers' formation we synthesized the $NaCNBH_3 \cdot THEC$ complex **2**. With a significantly lower basicity than BH_4^-, the $CNBH_3^-$ ion was expected to form weaker dihydrogen bonds.[4c,6] In fact, the crystal structure of **2** reveals the absence of any OH···HB close contacts, the cyanoborohydride ions participating in conventional hydrogen bonding through the N atoms. Notably, instead of forming dimers in this case the Na-THEC units self-assemble into extended helices through bifurcated OH···N···HO hydrogen bonds involving the CN groups (Figure 2). It thus appears that

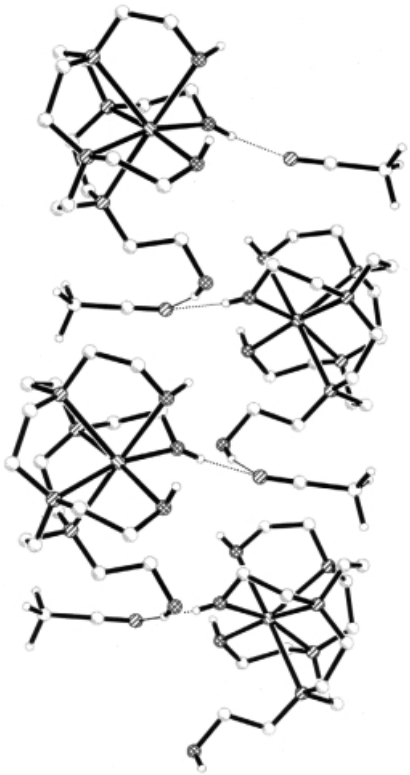

Figure 2. Helix formation by $NaCNBH_3 \cdot THEC$ (**2**) in the solid state.

  0947-6539/02/0801-0303 $ 17.50+.50/0

the OH···HB dihydrogen bonds play a central role in the formation of the dimers, as their absence resulted in a completely different supramolecular organization in **2**.[7]

$NaBH_4 \cdot$THPC (**3**) (THPC = 1,4,7,10-tetrakis((*S*)-2-hydroxypropyl)-1,4,7,10-tetraazacyclododecane)[8] was synthesized to explore the effect of subtle molecular modifications in the

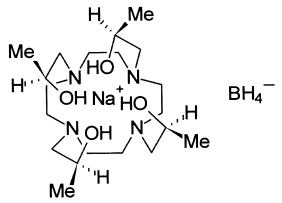

3

ligand upon dimer formation in the solid state. The complex precipitates as a white crystalline solid upon mixing $NaBH_4$ and THPC in 2-propanol. Its crystal structure is presented in Figure 3. The most notable feature is the formation of

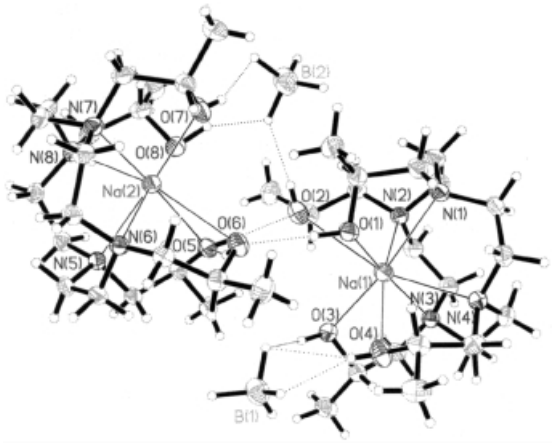

Figure 3. X-ray crystal structure of $NaBH_4 \cdot$THPC (**3**); dihydrogen bonding parameters [Å, °]: O(4)H···HB(1) (lower) 2.106, O(4)H···HB(1) (upper) 2.266, O(3)H···HB(1) 2.005, O(7)H···HB(2) 1.927, O(8)H···HB(2) 1.676, O(2)H···HB(2) 1.904, O(4)H–H–B(1) (lower) 96.1, O(4)H–H–B(1) (upper) 88.7, O(3)H–H–B(1) 113.8, O(7)H–H–B(2) 110.7, O(8)H–H–B(2) 120.2, O(2)H–H–B(2) 133.3, O(4)–H–HB(1) (lower) 162.5, O(4)–H–HB(1) (upper) 143.9, O(3)–H–HB(1) 153.4, O(7)–H–HB(2) 155.4, O(8)–H–HB(2) 153.0, O(2)–H–HB(2) 169.3.

hydrogen-bonded dimers, which display an S-shaped architecture as opposed to the O-shaped one in **1**. The most probable cause of this difference is the steric repulsion between the methyl groups, which would likely arise in an O-shaped dimer of **3**. The two THPC units in the dimer are held together by O(1)H···O(6) and O(5)H···O(2) conventional hydrogen bonds, as well as by O(7)H···HB(2)H···HO(2) and O(8)H···HB(2)H···HO(2) dihydrogen bonds. The second borohydride anion interacts with the remaining O(3)H and O(4)H from one THPC ligand.

More profound structural variations in the basic THEC supramolecular building block were brought about by replacing one of the hydroxyethyl arms with a 9-methylanthracyl group. The intention was to test the ability of the resulting functionalized ligand to maintain the association in dimers. Recurrence of this supramolecular motif would ultimately open the way to extended networks, by simple attachment of the tris-2-hydroxyethyl-cyclen units to appropriate spacers, using the remaining N atoms. The 9-[(1′,4′,7′-tris-2-hydroxyethyl-cyclen)]methylanthracene ligand (**4**) was synthesized from 9-(1′,4′,7′,10′-tetraazacyclododecyl)methylanthracene[9] and ethylene oxide [Eq. (1)], and its X-ray structure is

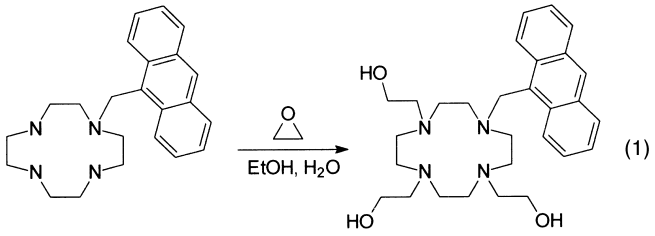

(1)

4

illustrated in Figure 4. Upon mixing with $NaBH_4$ in 2-propanol, complex $NaBH_4 \cdot$**4**$\cdot$2-propanol (**5**$\cdot$2-propanol) was formed, which precipitated as a white crystalline solid. However, recrystallization from acetonitrile/diethyl ether

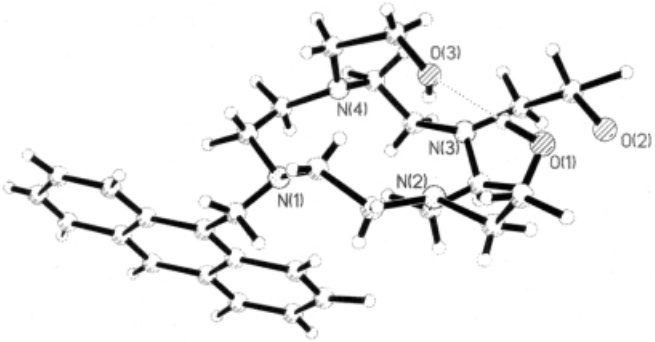

Figure 4. X-ray crystal structure of 9-(1′,4′,7′-tris-hydroxyethyl-cyclen)methylanthracene (**4**).

afforded single crystals incorporating disordered diethyl ether. Once again, self-assembly in dihydrogen-bonded dimers was revealed by X-ray crystallography (Figure 5). In contrast to the previous structures, no O–H···O interaction is present in this case; instead, the BH_4^- ions are intercalated

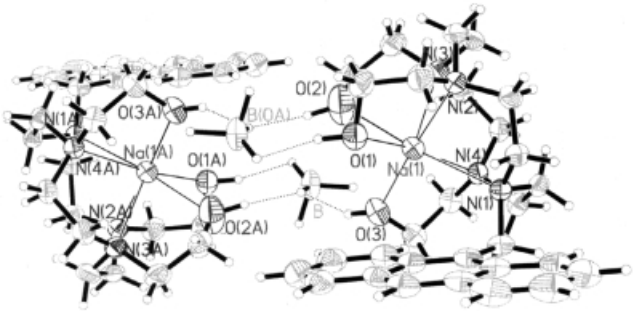

Figure 5. X-ray crystal structure of **5**$\cdot$$Et_2O$; normalized dihydrogen bonding parameters [Å, °]: O(1)H···HB 1.692, O(2)H···HB 1.661, O(3)H···HB 1.730, O(1)H···H–B 114.5, O(2)H···H–B 117.8, O(3)H···H–B 116.1, O(1)–H···HB 166.8, O(2)–H···HB 155.1, O(3)–H···HB 154.6.

0947-6539/02/0801-0304 $ 17.50+.50/0 *Chem. Eur. J.* **2002**, *8*, No. 1

between the two ligands, forming three dihydrogen bonds with the OH groups.

All of these examples demonstrate that various poly-HEC ligands persistently self-assemble into dihydrogen-bonded dimers in the presence of $NaBH_4$. Despite the fact that the exact connectivity of the dimers varies from one case to another in response to structural modifications in the ligand, the consistent recurrence of the general dimeric motif suggested to us that these dihydrogen-bonded units might be sufficiently reliable building blocks for the controlled assembly of extended networks. With this objective in mind, we synthesized ligand **6** with two tris-HEC units connected by a rigid *p*-xylylene spacer (Scheme 2), which we anticipated

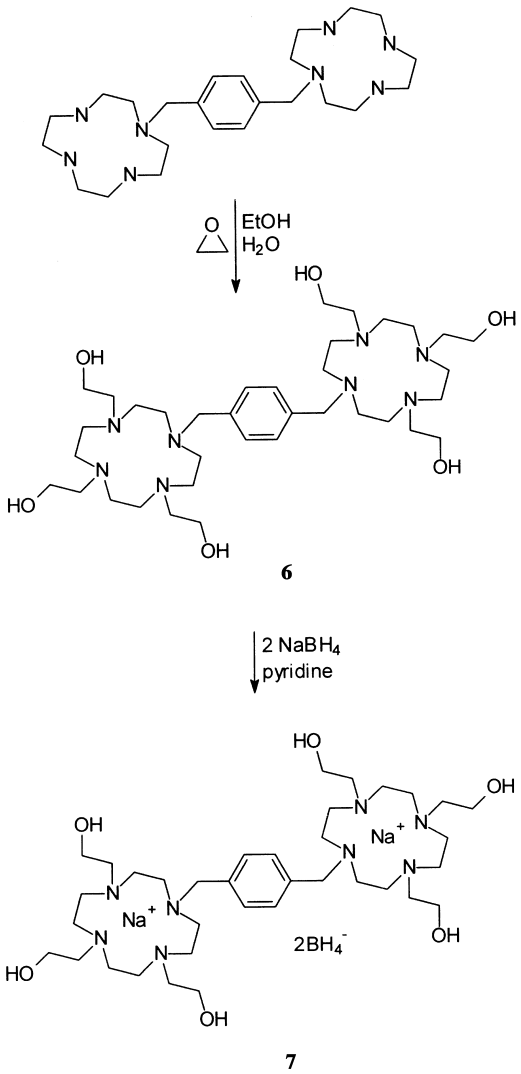

Scheme 2.

would self-assemble into one-dimensional chains in the presence of $NaBH_4$. Upon mixing **6** with sodium borohydride in a 1:2 ratio in pyridine, complex $2\,NaBH_4 \cdot \mathbf{6} \cdot$ pyridine (**7**·pyridine) was formed, whose X-ray crystal structure is depicted in Figure 6. As in the previous structures, complexation by Na^+ preorganizes the hydroxyethyl arms on the same face of the azacrown ring, thus favoring the self-association of

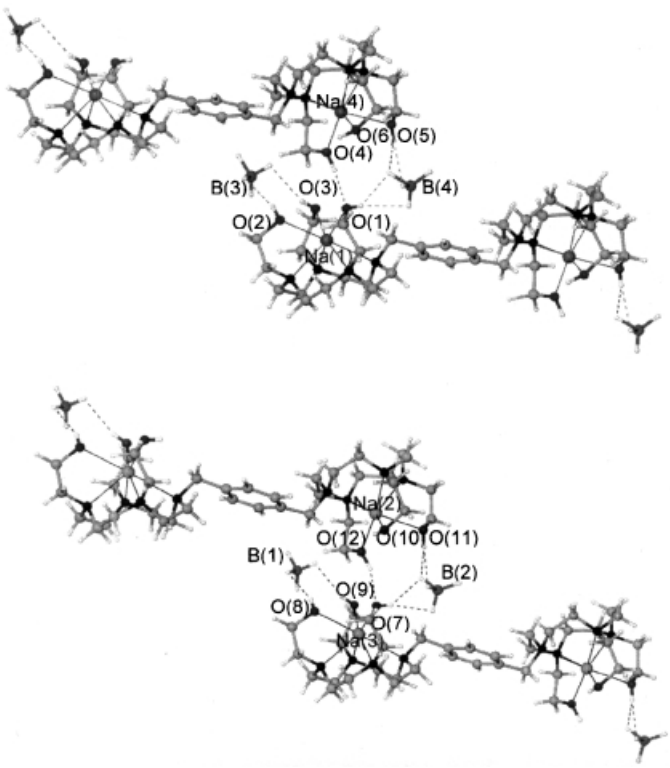

Figure 6. X-ray crystal structure of **7**·pyridine showing the two independent dihydrogen-bonded chains; dihydrogen bonding parameters [Å, °]: O(5)H···HB(4) (front) 2.245, O(5)H···HB(4) (back) 2.198, O(1)H···HB(4) (lower) 2.243, O(1)H···HB(4) (upper) 2.076, O(2)H···HB(3) 2.093, O(3)H···HB(3) 2.294, O(6)H···HB(3) 2.269, 2.303, O(11)H···HB(2) (front) 1.996, O(11)H···HB(2) (back) 2.216, O(7)H···HB(2) (lower) 2.095, O(7)H···HB(2) (upper) 2.092, O(8)H···HB(1) 2.218, O(9)H···HB(1) 2.174, O(10)H···HB(1) 2.373, O(5)H···H–B(4) (front) 82.88, O(5)H···H–B(4) (back) 89.99, O(1)H···H–B(4) (lower) 92.94, O(1)H···H–B(4) (upper) 91.52, O(2)H···H–B(3) 110.14, O(3)H···H–B(3) 100.53, O(6)H···H–B(3) 73.81, 73.83, O(11)H···H–B(2) (front) 94.16, O(11)H···H–B(2) (back) 83.09, O(7)H···H–B(2) (lower) 94.63, O(7)H···H–B(2) (upper) 92.55, O(8)H···H–B(1) 111.71, O(9)H···H–B(1) 107.49, O(10)H···H–B(1) 86.90, O(5)–H···HB(4) (front) 136.70, O(5)–H···HB(4) (back) 170.91, O(1)–H···HB(4) (lower) 163.86, O(1)–H···HB(4) (upper) 141.95, O(2)–H···HB(3) 160.28, O(3)–H···HB(3) 159.45, O(6)–H···HB(3) 144.00, 139.60, O(11)–H···HB(2) (front) 123.92, O(11)–H···HB(2) (back) 135.75, O(7)–H···HB(2) (lower) 166.56, O(7)–H···HB(2) (upper) 142.26, O(8)–H···HB(1) 156.37, O(9)–H···HB(1) 163.39, O(10)–H···HB(1) 140.19.

the tris-HEC moieties in dimers through the borohydride anions. The *p*-xylylene spacers interconnect the resulting dimeric units into extended chains. There are two crystallographically unique molecules of **7** in the unit cell, differing in their hydrogen bond parameters. In the first case, one BH_4^- connects neighboring tris-HEC units by dihydrogen bonding to O(1)H and O(5)H, generating one-dimensional chains. Additionally, conventional O(4)H···O(1) hydrogen bonds also provide intrachain connections. The second BH_4^- cross-links adjacent chains into two-dimensional layers by dihydrogen bonding to the O(2)H, O(3)H, and O(6)H groups. A similar self-assembly into extended chains, further associated in layers, is exhibited by the second unique molecule of **7**. In this case, O(7)H···HB(2) and O(11)H···HB(2) dihydrogen bonds, as well as O(12)H···O(7) interactions interconnect the tris-HEC units, while dihydrogen bonds between $B(1)H_4^-$ and

O(8)H, O(9)H, and O(10)H link the chains into layers. The shape of **7**, consisting of a long linear axis capped with bulky tris-HEC groups (wheel-and-axle),[10] precludes the close packing of the *p*-xylylene spacers within each layer, which leads to the formation of one-dimensional channels along the crystal, which are occupied by pyridine solvent (Figure 7). When **7** was recrystallized from pyridine-benzene, inclusion of the latter solvent occurred, as demonstrated by ^{1}H NMR spectroscopy.[11] The virtually identical powder X-ray diffraction patterns found for the pyridine and benzene clathrates indicate similar crystal structures for the two inclusion compounds.

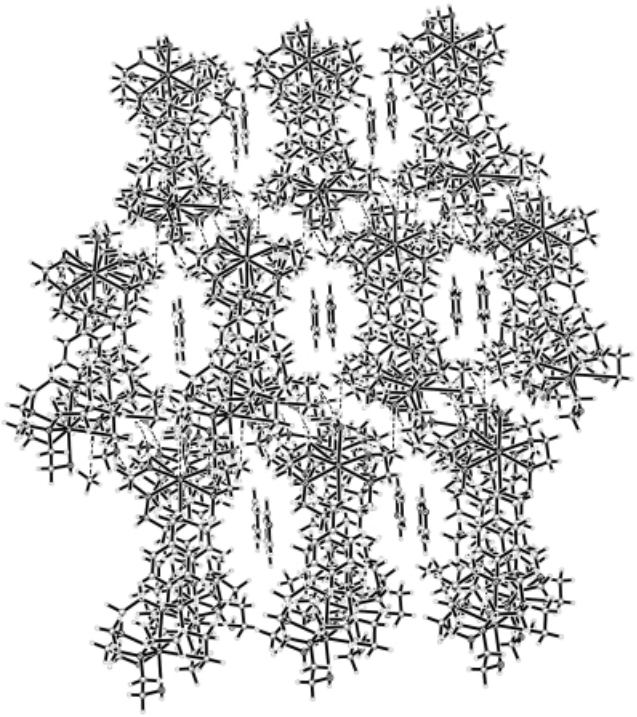

Figure 7. Crystal packing of **7**·pyridine showing the formation of extended channels occupied by the pyridine guest.

These dihydrogen-bonded inclusion complexes are particularly attractive, as they might lead to porous two-dimensional covalent networks upon topochemical loss of H_2. Such structures are expected to show enhanced stability, possibly comparable with that found in inorganic zeolites. More importantly, these materials could easily be functionalized by taking advantage of the residual $(RO)_xBH_{4-x}$ groups resulting from the solid-state decomposition.[12] However, preliminary experiments indicate that the benzene clathrate of **7** decomposes upon heating in the solid state with loss of H_2 and C_6H_6, unfortunately leading to the formation of an amorphous nonporous solid, insoluble in common solvents.[13] We are presently exploring the possibility of inducing the H_2 loss and B–O covalent bond formation prior to the evacuation of included benzene, which would ideally template the formation of a porous crystalline product. Alternatively, we consider other less volatile aromatic guests for serving the same purpose. Such studies have a top priority in our research agenda, as they could lead to the development of truly functional organic zeolites.

In summary, we have illustrated a strategy for building dihydrogen-bonded networks with architectures that can be controlled to a significant extent. Considering the high degree of flexibility in our building blocks, it is unrealistic to expect absolute predictability of the hydrogen bonding connectivity in these systems. By using appropriate spacers as in **7**, however, we anticipate that other extended dihydrogen-bonded and ultimately covalent frames will become accessible through rational design.

Experimental Section

Common chemicals and solvents were purchased from commercial sources and used without further purification. Melting points were taken on a Thomas Hoover instrument and are uncorrected. FT-IR spectra were measured in KBr pellets on a Perkin Elmer Spectrum 2000 instrument. ^{1}H NMR (300.1 MHz) spectra were recorded on a Gemini-300 instrument. ^{13}C NMR (75.4 MHz) and ^{11}B NMR (96.23 MHz) spectra were recorded on a Varian VXR-300 instrument. ^{1}H and ^{13}C NMR chemical shifts were referenced to residual protons in the solvent, while the ^{11}B NMR chemical shifts were referenced to $B(OCH_3)_3$ in $CDCl_3$. X-ray powder diffraction measurements were conducted on a Rigaku–Denki RW400F2 diffractometer with monochromatic $Cu_{K\alpha}$ radiation, operated at 45 kV and 100 mA. Thermogravimetric analysis was recorded on a CAHN TGSystem 121 instrument at a heating rate of 5 °C min^{-1}.

X-ray structure determinations of 2, 3, 4, 5·Et$_2$O, and 7·pyridine (Table 1): X-Ray crystallographic measurements were carried out on a Siemens SMART CCD diffractometer with graphite-monochromated $Mo_{K\alpha}$ radiation ($\lambda = 0.71073$ Å), operated at 50 kV and 40 mA. The structures were solved by direct methods and refined on F^2 using the SHELXTL software package.[14] Absorption corrections were applied using SADABS, part of the SHELXTL software package. All non-hydrogen atoms were refined anisotropically. Hydrogen atoms were generally located from difference Fourier maps and refined isotropically. For the $B(2)H_4^-$ in **3**, however, only the hydridic hydrogen atoms involved in dihydrogen bonding could be found; the two noninteracting hydridic hydrogen atoms were calculated, and the four hydrogen atoms were subsequently constrained in an idealized tetrahedral geometry, with B–H distances of 1.21 Å. Also, the B–H hydridic and O–H protonic hydrogen atoms in **5**, although easily located from the difference Fourier maps, yielded O–H···H–B contact distances that were unrealistically short, and therefore the observed O–H and B–H distances were normalized to ideal values of 0.96 and 1.21 Å, respectively. The pyridine hydrogen atoms in **7**·pyridine were calculated and placed in idealized positions. The O(2) atom in **4** and the inclusion ether in **5**·Et$_2$O showed significant disorder, and consequently no attempts were made to locate or calculate their corresponding hydrogen atoms.

Crystallographic data (excluding structure factors) for the structures reported in this paper have been deposited with the Cambridge Crystallographic Data Center as supplementary publications nos. CCDC-166694 (**2**), CCDC-166695 (**3**), CCDC-166696 (**4**), CCDC-166697 (**5**·Et$_2$O), CCDC-166698 (**7**·pyridine). Copies of the data can be obtained free of charge on application to CCDC, 12 Union Road, Cambridge CB2 1EZ, UK (fax: (+44) 1223-336033; e-mail: deposit@ccdc.cam.ac.uk).

NaCNBH$_3$·THEC (2): $NaCNBH_3$ (0.032 g, 0.5 mmol) in THF (3 mL) was added to THEC·H_2O (0.183 g, 0.5 mmol) in THF. A white precipitate formed immediately. The mixture was stirred for 1 h at room temperature under an argon atmosphere. The solid was subsequently filtered and washed with THF to yield 0.17 g (83%) of **2**. Single crystals suitable for X-ray crystallography were grown by diffusion of Et_2O into a solution of **2** in CH_3CN. M.p. 230–234 °C (decomp); ^{1}H NMR (CD_3CN): $\delta = 3.61$ (t, $J =$ 4.8 Hz, 8H; OCH_2), 3.25 (br s, 4H; OH), 2.47 (br, 24H; NCH_2), 0.25 (q, 3H; $NCBH_3$); ^{13}C NMR (CD_3CN): $\delta = 51.17$ (NCH_2), 56.50 (NCH_2), 59.06 (OCH_2); ^{11}B NMR (CD_3CN): $\delta = -56.60$ (q, $J_{B,H} = 88.3$ Hz; $NCBH_3$); IR (KBr): $\nu_{BH} = 2348$, $\nu_{CN} = 2162$ cm^{-1}.

NaBH$_4$·THPC (3): THPC[8] (0.285 g, 0.7 mmol) was added to a solution of $NaBH_4$ (0.027 g, 0.7 mmol) in 2-propanol (8 mL). Within approximately 2 min a white precipitate formed. The mixture was left standing for 1 h at

  0947-6539/02/0801-0306 $ 17.50+.50/0 *Chem. Eur. J.* **2002**, *8*, No. 1

room temperature, then the solid was filtered. Yield 0.085 g (27%). No melting occurs when the solid is heated up to 200 °C, at which temperature it turns brown, and eventually starts to melt at approximately 210 °C. Single crystals suitable for X-ray crystallography were grown by slow evaporation of a 2-propanol solution. ^{1}H NMR (D_2O): $\delta = 3.89$ (br m, 4H; OCH), 2.90–2.87 (br, 8H; NCH_2), 2.42–2.34 (br, 4H; NCH_2), 2.09 (br, 12H; NCH_2), 0.98 (d, 12H; CH_3), −0.27 (q, $J_{B,H} = 80.7$ Hz, 4H; BH_4); ^{13}C NMR ([D_6]DMSO): $\delta = 21.79$ (CH_3), 49.17 (NCH_2), 51.03 (NCH_2), 61.58 (NCH_2), 62.31 (OCH_2); ^{11}B NMR ([D_6]DMSO): δ −52.55 (quintet, $J_{B,H} = 82.8$ Hz; BH_4); IR (KBr): $\nu_{BH} = 2290$ cm^{-1}; elemental analysis calcd (%) for $C_{20}H_{48}N_4O_4BNa$: C 54.30, H 10.86, N 12.67; found: C 54.66, H 11.39, N 12.41.

9-(1′,4′,7′-Tris-hydroxyethyl-cyclen)methylanthracene (4): **Warning**: Ethylene oxide is a volatile (b.p. = 11 °C), extremely toxic, and carcinogenic substance. 9-(1′,4′,7′,10′-Tetraazacyclododecyl)methylanthracene[9] (0.2 g, 0.57 mmol) was dissolved in absolute ethanol (3 mL). Water (2 mL) was added, and the solution was cooled to 0 °C. Ethylene oxide (0.158 g, 3.6 mmol) was cooled to 0 °C and was added to the reaction mixture, which was stirred at 0 °C for 2 h, followed by an additional hour of stirring at room temperature. Solvent evaporation under vacuum at 35 °C yielded a yellow oil. A few mL of water were subsequently added, and the resulting aqueous solution was extracted with chloroform. Evaporation of $CHCl_3$ yielded a yellow oil, which was dissolved in minimal amount of 2-propanol, and a large excess of Et_2O was added. Upon standing in the freezer over night, a yellow crystalline solid precipitated, which was filtered and washed with Et_2O, to give **4** (0.12 g; 42%). Single crystals suitable for X-ray crystallography were grown by diffusion of Et_2O into a solution of **4** in 2-propanol. M.p. 131–133 °C; ^{1}H NMR (CD_3Cl): $\delta = 8.36$ (d, 2H; ArH), 8.29 (s, 1H; ArH), 7.87 (d, 2H; ArH), 7.38 (m, 4H; ArH), 4.8 (br; OH), 4.39 (s, 2H; $ArCH_2$), 3.47 (t, $J = 4.5$ Hz, 2H; OCH_2), 3.40 (t, $J = 4.5$ Hz, 4H; OCH_2), 2.73 (t, $J = 4.5$ Hz, 6H; NCH_2), 2.43–2.32 (br, 16H; NCH_2); ^{13}C NMR (CD_3Cl): $\delta = 130.83$, 128.51, 127.11, 125.32, 124.50, 58.35, 58.01, 57.73, 55.65, 52.37, 52.11, 51.90, 50.88, 50.56; elemental analysis calcd (%) for $C_{29}H_{42}N_4O_3$: C 70.45, H 8.50, N 11.34; found: C 70.23, H 8.83, N 11.04.

$NaBH_4 \cdot$ [9-(1′,4′,7′-tris-hydroxyethyl-cyclen)methylanthracene] · *i*PrOH (5 · 2-propanol): 9-(1′,4′,7′-Tris-hydroxyethyl-cyclen)methylanthracene (**4**) (0.1 g, 0.2 mmol) was added to a solution of $NaBH_4$ (0.008 g, 0.21 mmol) in 2-propanol (4 mL). Within approximately 4 min a white precipitate formed. The mixture was stirred 2 h at room temperature under an argon atmosphere, and subsequently filtered to give **5** · 2-propanol (0.09 g; 53%). The solid turns red when heated, and partly melts at 190 °C. Single crystals suitable for X-ray crystallography were grown by diffusion of Et_2O into a solution of **5** in CH_3CN. ^{1}H NMR (CD_3CN): $\delta = 8.54$ (s, 1H; ArH), 8.43 (d, 2H; ArH), 8.06 (d, 2H; ArH), 7.60 (m, 2H; ArH), 7.49 (m, 2H; ArH), 4.61 (s, 2H; $ArCH_2$), 3.72 (septet, 1H; *i*PrOH), 3.6–1.9 (br), 1.08 (d, 6H; *i*PrOH); −0.18 (q, $J_{B,H} = 81.3$ Hz, 4H; BH_4) ^{13}C NMR (CD_3CN): $\delta =$ 132.47, 130.23, 128.98, 127.77, 126.22, 125.46, 58.54, 57.98, 56.54, 56.15, 54.51, 52.65, 51.59, 51.26, 50.74; ^{11}B NMR (CD_3CN): $\delta = -53.75$ (quintet, $J_{B,H} = 80.4$ Hz; BH_4); IR (KBr): $\nu_{BH} = 2384$, 2293, 2228 cm^{-1}; elemental analysis calcd (%) for $C_{32}H_{54}N_4O_4NaB$: C 64.87, H 9.12, N 9.46; found: C 64.20, H 9.06, N 9.33.

***p*-Xylylene-bis[(1′,4′,7′-tris-hydroxyethyl)-cyclen)] (6)**: Water (2.5 mL) was added to a solution of *p*-xylylene-bis-cyclen[15] (0.35 g, 0.78 mmol) in absolute ethanol (2.5 mL). The resulting slightly turbid solution was cooled to 0 °C, and ethylene oxide (0.41 g, 9.3 mmol) was subsequently added. The mixture was magnetically stirred at 0 °C for 4 h, which resulted in the formation of a white precipitate. After the removal of ethanol and excess ethylene oxide in vacuo at room temperature, the precipitate was collected by filtration, yielding **6** (0.25 g; 45%). M.p. 144–147 °C; ^{1}H NMR ($CDCl_3$): $\delta = 7.27$ (s, 4H; ArH), 5.2 (br; OH), 3.59, 3.58 (br, 16H; $ArCH_2$, OCH_2), 2.56, 2.46 (br, 44H; NCH_2); ^{13}C NMR ($CDCl_3$): $\delta = 136.68$, 129.20, 59.51, 59.02, 58.79, 56.90, 56.20, 52.30, 52.24, 51.30, 51.25; elemental analysis calcd (%) for $C_{36}H_{70}N_8O_6$: C 60.81, H 9.92, N 15.76; found: C 60.51, H 10.47, N 15.62.

$2\,NaBH_4 \cdot$ {*p*-xylylene-bis[(1′,4′,7′-tris-hydroxyethyl)-cyclen)]} · C_6H_6 (7 · benzene): Compound **6** (0.15 g, 0.21 mmol) and $NaBH_4$ (0.016 g, 0.42 mmol) were dissolved in pyridine (5 mL). Slow evaporation of the solvent under an argon atmosphere yielded a few crystals of **7** · pyridine and a yellow oil. This mixture was redissolved in 0.5 mL pyridine, and benzene (15 mL) was added. The resulting solution was placed in the freezer for 20 min, then warmed to room temperature. The crystallized complex was filtered and washed with benzene. Yield 0.14 g. ^{1}H NMR (CD_3CN): $\delta =$ 7.36, 7.29 (s, C_6H_6; ArH), 3.66, 3.57 (br, 16H; $ArCH_2$, OCH_2), 2.47, 2.26 (br, 44H; NCH_2), −0.26 (q, $J_{B,H} = 81.3$ Hz, 8H; BH_4); ^{13}C NMR (CD_3CN): $\delta =$ 136.60, 131.11, 129.29, 59.67, 58.38, 56.06, 55.91, 51.51, 50.56, 50.44; ^{11}B NMR (CD_3CN) δ −53.46 (quintet, $J_{B,H} = 81.4$; BH_4); IR (KBr): $\nu_{BH} =$ 2295 cm^{-1}.

Acknowledgements

This work was supported in part by the MSU Center for Fundamental Materials Research (CFMR). Support from the Harold Hart endowed fellowship (summer, 2000) is also gratefully acknowledged by R.C.

Table 1. Crystallographic data for **2**, **3**, **4**, **5** · Et_2O, and **7** · pyridine.

	2	**3**	**4**	**5** · Et_2O	**7** · pyridine
formula	$C_{17}H_{39}N_5O_4BNa$	$C_{20}H_{48}N_4O_4BNa$	$C_{29}H_{42}N_4O_3$	$C_{33}H_{56}N_4O_4BNa$	$C_{41}H_{83}N_9O_6B_2Na_2$
formula weight	411.33	442.42	494.67	590.62	865.76
color	colorless	colorless	pale yellow	pale yellow	colorless
dimensions [mm]	0.65 × 0.29 × 0.26	0.49 × 0.41 × 0.18	0.39 × 0.18 × 0.08	0.49 × 0.18 × 0.13	0.23 × 0.15 × 0.10
crystal system	orthorhombic	monoclinic	triclinic	monoclinic	triclinic
space group, Z	$Pna2_1$, 4	$P2_1$, 4	$P\bar{1}$, 2	$P2_1/n$, 4	$P\bar{1}$, 4
a [Å]	25.2624(3)	9.7915(4)	8.7352(3)	12.7329(6)	10.3858(5)
b [Å]	9.4053(2)	18.1449(7)	12.2971(4)	19.0589(2)	15.4021(8)
c [Å]	9.4430(2)	14.6111(6)	13.7789(3)	13.7260(6)	34.091(2)
α [°]	90	90	69.152(2)	90	80.7830(10)
β [°]	90	96.867(2)	79.456(2)	95.459(2)	81.2410(10)
γ [°]	90	90	78.736(2)	90	70.2950(10)
V [Å^3]	2243.66(7)	2577.27(18)	1346.11(7)	3315.8(2)	5039.3(5)
T [K]	173(2)	173(2)	173(2)	173(2)	173(2)
ρ_{calcd} [g cm^{-3}]	1.218	1.140	1.220	1.183	1.141
reflections collected	22515	23846	12550	30419	39463
unique reflections	5336	11681	6195	7907	17650
$2\theta_{max}$ [°]	56.40	56.48	56.54	56.50	50
no. of parameters	410	923	489	541	1706
R_1[a], wR_2[b]	0.0251, 0.0637	0.0358, 0.0968	0.0825, 0.2187	0.0672, 0.1646	0.0732, 0.1590
residual electron density [e Å^{-3}]	0.205	0.517	1.571	0.767	0.484
goodness of fit	1.022	0.789	1.268	1.027	0.971

[a] $R_1 = \Sigma(|F_0| - |F_c|)/\Sigma|F_0|$. [b] $wR_2 = \{\Sigma[w(F_0^2 - F_c^2)^2]/\Sigma[w(F_0^2)^2]\}^{1/2}$.

[1] a) G. M. Whitesides, E. E. Simanek, J. P. Mathias, C. T. Seto, D. N. Chin, M. Hammen, D. M. Gordon, *Acc. Chem. Res.* **1995**, *28*, 37; b) X. Wang, M. Simard, J. D. Wuest, *J. Am. Chem. Soc.* **1994**, *116*, 12119; c) K. T. Holman, S. M. Martin, D. P. Parker, M. D. Ward, *J. Am. Chem. Soc.* **2001**, *123*, 4421; d) R. E. Melendez, A. J. Carr, B. R. Linton, A. D. Hamilton, *Struct. Bond.* **2000**, *96*, 31; e) M. J. Zaworotko, *Chem. Commun.* **2001**, 1; f) A. Nangia, G. R. Desiraju, *Top. Curr. Chem.* **1998**, *198*, 57; g) J. W. Lauher, F. W. Fowler, *J. Phys. Org. Chem.* **2000**, *13*, 850; h) D. Braga, F. Grepioni, *Acc. Chem. Res.* **2000**, *33*, 601; i) M. Mazik, D. Blaser, R. Boese, *Chem. Eur. J.* **2000**, *6*, 2865; j) R. Bishop, *Synlett,* **1999**, *9*, 1351; k) S. V. Kolotuchin, P. A. Thiessen, E. E. Fenlon, S. R. Wilson, C. J. Loweth, S. C. Zimmerman, *Chem. Eur. J.* **1999**, *5*, 2537; l) J. C. M. Rivas, L. Brammer, *Coord. Chem. Rev.* **1999**, *183*, 43; m) P. C. Andrews, M. J. Hardie, C. L. Raston, *Coord. Chem. Rev.* **1999**, *89*, 169; n) L. R. MacGillivray, J. L. Atwood, *J. Solid State Chem.* **2000**, *152*, 199; o) M. J. Krische, J. M. Lehn, *Struct. Bond.* **2000**, *96*, 3; p) C. B. Aakeroy, *Acta Crystalloggr. B*, **1997**, *53*, 569; r) J. H. K. K. Hirschberg, L. Brunsveld, A. Ramzi, J. A. J. M. Vekemans, R. P. Sijbesma, E. W. Meijer, *Nature* **2000**, *407*, 167; s) D. T. Bong, T. D. Clark, J. R. Granja, M. R. Ghadiri, *Angew. Chem.* **2001**, *113*, 1016; *Angew. Chem. Int. Ed.* **2001**, *40*, 988; t) L. J. Prins, D. N. Reinhoudt, P. Timmerman, *Angew. Chem.* **2001**, *113*, 2446; *Angew. Chem. Int. Ed.* **2001**, *40*, 2382.

[2] a) R. Custelcean, J. E. Jackson, *Chem. Rev.* **2001**, *101*, 1963; b) M. J. Calhorda, *Chem. Commun.* **2000**, 801; c) R. H. Crabtree, P. E. M. Siegbahn, O. Eisenstein, A. L. Rheingold, T. F. Koetzle, *Acc. Chem. Res.* **1996**, *29*, 348; d) E. S. Shubina, N. V. Belkova, L. M. Epstein, *J. Organomet. Chem.* **1997**, *536–537*, 17; e) K. Abdur-Rashid, D. G. Gusev, A. L. Lough, R. H. Morris, *Organometallics* **2000**, *19*, 834; f) D. Braga, P. De Leonardis, F. Grepioni, E. Tedesco, M. J. Calhorda, *Inorg. Chem.* **1998**, *37*, 3337.

[3] J. P. Campbell, J. W. Hwang, V. G. Young, R. B. Von Dreele, C. J. Cramer, W. L. Gladfelter, *J. Am. Chem. Soc.* **1998**, *120*, 521.

[4] a) R. Custelcean, M. Vlassa, J. E. Jackson, *Angew. Chem.* **2000**, *112*, 3437; *Angew. Chem. Int. Ed.* **2000**, *39*, 3299; b) R. Custelcean, J. E. Jackson, *J. Am. Chem. Soc.* **2000**, *122*, 5251; c) R. Custelcean, J. E. Jackson, *J. Am. Chem. Soc.* **1998**, *120*, 12935; d) R. Custelcean, J. E. Jackson, *Angew. Chem.* **1999**, *111*, 1748; *Angew. Chem. Int. Ed.* **1999**, *38*, 1661; e) J. W. Hwang, J. P. Campbell, J. Kozubowski, S. A. Hanson, J. F. Evans, W. L. Gladfelter, *Chem. Mater.* **1995**, *7*, 517.

[5] S. L. Whitbread, A. Politis, A. K. W. Stephens, J. B. Lucas, R. S. Dhilon, S. F. Lincoln, K. P Wainwright, *J. Chem. Soc. Dalton Trans.* **1996**, 1379.

[6] R. Custelcean, *J. Mol. Struct. Theochem* **2000**, *505*, 95.

[7] The dimers are also absent in the reported complex NaSCN · THEC, whose crystal structure is very similar with the one found in **2** (P. Groth, *Acta Chem. Scand.* **1983**, *A 37*, 283). Interestingly, however, the analogous KSCN · THEC complex self-assembles in dimers, which display a very close connectivity to the one observed in **1**. These facts suggest that there is a very delicate balance of cation – THEC – anion interactions, which determines the presence or absence of dimers.

[8] R. S. Dhillon, S. E. Madbak, F. G. Ciccone, M. A. Buntine, S. F. Lincoln, K. P. Wainwright, *J. Am. Chem. Soc.* **1997**, *119*, 6126.

[9] E. U. Akkaya, M. E. Huston, A. W. Czarnik, *J. Am. Chem. Soc.* **1990**, *112*, 3590.

[10] a) R. K. R. Jetti, F. Xue, T. C. W. Mak, A. Nangia, *J. Chem. Soc. Perkin Trans. 2*, **2000**, 1223; b) R. Bishop, *Chem. Soc. Rev.* **1996**, 311.

[11] Inclusion of 0.6 – 0.7 mol C_6H_6 and no pyridine was indicated by the ^{1}H NMR spectrum.

[12] Investigation of the solid state decomposition product from a previously studied dihydrogen-bonded network[4b] indicated that the resulting polyalkoxyborohydride groups can easily react with $Pd(OAc)_2$ to generate polymer-supported Pd^0 centers; R. Custelcean, Ph. D. Dissertation, Michigan State University, **2000**.

[13] Thermogravimetric analysis shows a weight loss corresponding to both included benzene and 6 mol of H_2, between room temperature and 300 °C. Additionally, upon heating **7** · benzene in the solid state at 160 °C for 24 h, disappearance of the initial ν_{BH} band at 2295 cm^{-1} and the appearance of a new one at 2373 cm^{-1} were observed by IR spectroscopy.

[14] SHELXTL: Structure Analysis Program 5.1; Bruker AXS, Inc., Madison, WI, **1997**.

[15] T. Koike, M. Takashige, E. Kimura, H. Fujioka, M. Shiro, *Chem. Eur. J.* **1996**, *2*, 617.

Received: July 16, 2001 [F3419]

  0947-6539/02/0801-0308 $ 17.50+.50/0